

RYSZARD WÓJTOWICZ¹, PAWEŁ WOLAK²

AN EXAMPLE OF THE USE OF COMPUTATIONAL-FLUID-DYNAMICS ANALYSIS FOR SIMULATION OF TWO-PHASE FLOW IN A CYCLONE WITH A TANGENTIAL INLET

The feasibility of using a software package, based on computational fluid dynamics (CFD) codes to simulate two-phase (gas–solid) flows in a cyclone with a tangential inlet was studied. The methodology of numerical simulations and calculations has been presented and the main parameters influencing the effectiveness of the cyclone elaborated. Findings are presented as contour maps of the distribution of selected flow parameters (velocity, pressure) in some parts of the apparatus or as visualizations of vortex formation structures and particle motion trajectories in the cyclone. The results of simulation were compared with those based on literature correlations and experimental results of laboratory tests.

1. INTRODUCTION

Cyclones constitute a large group of devices commonly used in many industrial technologies. They are used for separation of solid particles from a dusty gas, mainly in processes of environmental protection [1, 2], and also as final separation devices in pneumatic transport systems. Cyclones have a simple and compact design, are devoid of moving parts, and their universality and uncomplicated operation make them perfectly adapted to work in various, often adverse conditions such as high pressure and elevated temperatures at variable humidity of polluted gas.

¹Cracow University of Technology, Faculty of Mechanical Engineering, Institute of Thermal and Process Engineering, Aleja Jana Pawła II 37, 31-864 Cracow, Poland, corresponding author: R. Wójtowicz. e-mail: rwojtowi@pk.edu.pl

²Air Liquide Global E&C Solutions, Poland S.A., Static Equipment Department, Mogilska 41, 31-545 Cracow, Poland.

Despite the simplicity of construction of the cyclone, its gas flow profile is complex and depends on several parameters, mainly influenced by geometry and dimensions of its parts. An essential significance have also the shape and location of the inlet of polluted gas and of an overflow pipe. Their accurate construction enables one to eliminate undesirable phenomena occurring during the operation such as gas flow directly from inlet to outlet duct of the cyclone (so-called short circuit), a violent contraction of the inlet stream or – impeding dust removal - transferring vortex motion of gas to a reservoir of dust.

Computer simulation packages based on specially created codes of computational fluid dynamics (CFD) [3–5] are useful tools commonly applied during computer-aided design of industrial equipment. Their advantages such as the universality of application, ability to quickly modify dimensions and geometry of a designed device and also broad possibility of presentation of results make them useful during design and optimization of dust separators including cyclones. An important advantage of their application seems to be the possibility of modeling of multiphase flows – in the case of cyclones a two-phase flow (gas–solid particles), being crucial in optimization of constructions and in the estimation of pressure drops, sizes of particles separated in the cyclone and effectiveness of its dedusting. Due to all those advantages, CFD packages seem to be useful and helpful in the analysis of cyclone separators. However, not many papers have been published on this topic.

Elsayed and Lacor [6] using CFD simulations and Muschelknautz's approach conducted optimization of the cyclone geometry (the vortex finder diameter, inlet width and height, and cyclone total height) for a minimum pressure drop. A new set of geometrical ratios for a cyclone design was proposed. Safikani et al. [7] presented the results of CFD simulations of flow field in three types of cyclones, named 1D3D, 2D2D and 1D2D. The length of the cylindrical part of the body is equal to 1, 2, and 1 the body diameters, while the length of the conical part is 3, 2 and 2 the body diameters. The authors analyzed velocities, static pressure and turbulence intensity distributions. Predicted data were compared to experimental as well as theoretical values. The impact of particle agglomeration on the collection efficiency of a cyclone was studied by Paiva et al. [8] and a new model for prediction of the collection efficiency was proposed. The maximum-efficiency cyclone length was found by Surmen et al. [9]. The authors, using a theoretical approach based on cyclone geometry and fluid properties obtained a relationship describing minimum particle diameter or maximum cyclone efficiency.

Few papers only were published on CFD modelling of cyclone separators, compared to many published studies on other industrial equipment, e.g. mixing vessels or heat exchangers. Many papers lack a comparison between CFD-predicted results, theoretically calculated values, and measurements. Even if two-phase simulations were performed – possibilities of CFD software for presentation of the results were relatively poorly used. The papers lack visualizations of flow, vortices formation etc., created on based on various defined criterions. In addition, the research lacks visualization of selected trajectories of particles and analysis their collection in main part of a cyclone as

well as in a dust chamber, which can help in selection and optimization of a cyclone design. The current state of research shows a need for further examination.

2. THE MECHANISM OF PARTICLE DEDUSTING IN A CYCLONE AND MAIN PARAMETERS DETERMINING EFFECTIVENESS OF ITS PERFORMANCE

In cyclones for gas dedusting, a more efficient dedusting mechanism is used, based on centrifugal forces acting on particles. A stream of a polluted gas is introduced tangentially into a cyclone. Next, a dusty gas set in a rotational motion creates in a cyclone the so-called the outer spiral with a diameter comparable to the cylindrical part of a cyclone diameter. Centrifugal force acting on particles causes their gradual movement in the direction of an apparatus wall and as a consequence, their collection. The purified gas forms the so-called inner spiral (a small-scale vortex close to the cyclone vertical axis) and escapes outside through the vortex finder. A centrifugal force which determines a particle dedusting process depends on the geometry and dimensions of the cyclone, particle size, and first of all on a tangential velocity of gas. For effective cyclone performance, these quantities must be taken into account at the stage of its design and during the choice of process conditions.

An analysis of motion of a dusty gas in a cyclone based on various models proposed in the literature leads to a choice of two main parameters determining an efficiency of cyclone performance, which are: pressure drop of gas flowing through a cyclone and dedusting efficiency. The pressure drop of gas in a cyclone can be caused by many factors, e.g. by gas frictional drags at an inlet and walls, also by energy losses during gas decompression and turbulence inside a cyclone. The latter parameter directly determines the selection of devices supplying a dusty gas to a cyclone and their power requirements, and therefore – which is important – energy expenditure for the whole process.

Correlations for determining the pressure drop in cyclones have a similar form and take into account an inlet gas velocity and geometry of an apparatus. This dependence in a general manner can be written as:

$$\Delta p = \alpha \frac{u^2}{2} \rho_c \quad (1)$$

where α is a coefficient characterized by a cyclone dimension proportion, variously defined by various authors.

Warych [2] characterized α as the coefficient of local resistance (ξ) and recommends to assume its value between 4.5 and 11.0, depending on the geometry of a cyclone. Casal and Martinez [10] on the basis of a statistical analysis of experimental data propose a correlation in the form of:

$$\alpha = 11.3 \left(\frac{ab}{D_e^2} \right)^2 + 3.33 \quad (2)$$

Another equation to determine the α coefficient was proposed by Shepherd and Lapple [11]:

$$\alpha = 16 \frac{ab}{D_e^2} \quad (3)$$

Coker [12] defined α as:

$$\alpha = 9.47 \frac{ab}{D_e^2} \quad (4)$$

Typical inlet velocities of a dusty gas for a cyclone amount to 10–25 m/s [1, 2]. However, the highest ones with substantial concentrations of particles in the gas can cause a strong erosion of the cyclone, in the upper, inlet part as well as in the lower, conical one.

The other important parameter characterizing the effectiveness of a cyclone performance is its dedusting efficiency η . A classic relation for estimation of dedusting efficiency can be written as:

$$\eta = \frac{m_s}{m_i} \times 100\% \quad (5)$$

where: m_s is a weight of dedusted (collected) particles, and m_i is a weight of all particles supplied to a cyclone with a polluted gas.

Another correlation was proposed by Leith and Licht [13]:

$$\eta_i = 1 - \exp \left[-2 \left(2(n+1) \tau_i \left(\frac{u}{R} \right)^2 t \right)^{1/(2n+2)} \right] \quad (6)$$

where: τ_i is a response time dependent on a particle diameter, particle density and gas viscosity, t represents an average residence time of gas depending on a gas inlet velocity and cyclone geometry, n is the so-called vortex exponent, calculated from the following equation:

$$n = 1 - \left(1 - 0.669 D^{0.14} \right) \left(\frac{T}{293} \right)^{0.3} \quad (7)$$

Taking above into account and analyzing the previously described relation of particle deposition with the value of a centrifugal force acting on particles, we can state that, dedusting efficiency will increase upon increasing particle diameter, their density and tangential velocity, while decrease upon increasing radius of particle swirl in an apparatus.

3. SIMULATION METHODOLOGY

Figure 1 presents a view, geometry and basic dimensions of the investigated cyclone. The diameter of the cylindrical part was $D = 0.192$ m, and the total height of the cyclone $H = 0.745$ m. The inlet channel was square cross-sectional, with dimensions $a = b = 0.042$ m and total length $c = 0.2$ m. The height of the cylindrical part of the cyclone was $h = 0.242$ m, the diameter of the vortex finder $D_e = 0.09$ m and length of the vortex finder inside the cyclone was $s = 0.140$ m. The diameter of the cyclone at the end of the conical part was chosen to be $B = 0.045$ m.

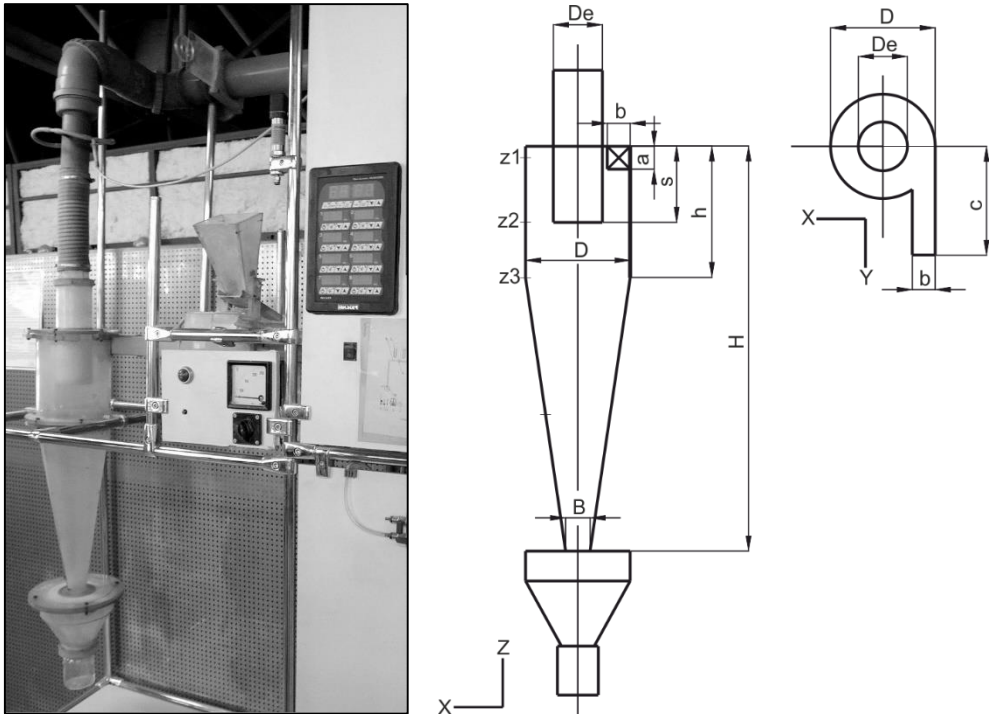


Fig. 1. The cyclone investigated: a) a general view, b) geometry and overall dimensions ($z1-z3$ – cross-section planes)

The gas flowing through the cyclone was air ($\rho_c = 1.225 \text{ kg/m}^3$, $\mu_c = 1.7894 \cdot 10^{-5} \text{ Pa}\cdot\text{s}$), its velocity u at the inlet of the cyclone was changed in the range of 10–20 m/s. The ash with density of $\rho_s = 2700 \text{ kg/m}^3$ was used as solid particles. The dispersed phase volume fraction was relatively low, lower than 5%. During simulations, it was assumed that particle size distribution is characterized by the Rosin–Rammler theoretical distribution (Fig. 2), whose main parameters are listed in Table 1. All parameters of particles assumed in simulations were the same as those in our laboratory tests used (verification of simulations).

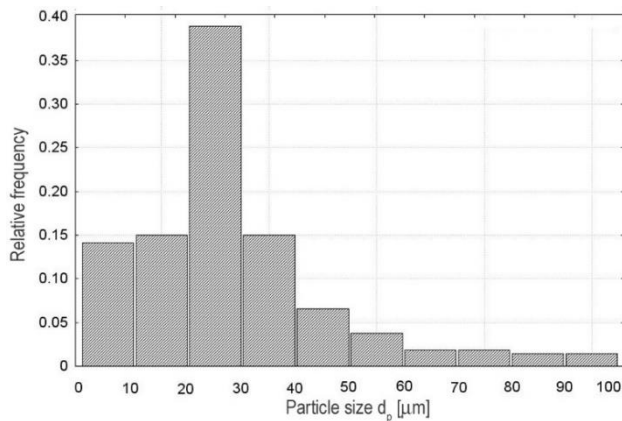


Fig. 2. Size distribution of applied particles

Table 1

Main statistical parameters of particle population

Parameter	Value
Total number of particles n	5.321×10^6
Minimum diameter $d_{p\min}$	2 μm
Maximum diameter $d_{p\max}$	100 μm
Mean diameter $d_{p\text{mn}}$	24.7 μm
Sauter mean diameter d_{32}	51.5 μm
Standard deviation σ	17.3 μm
Spread parameter β	2.537

The analysis of the two-phase (gas–solid) flow was performed based on results of numerical modelling, using as a pre-processor the mesh generator Gambit 2.4. At the pre-processing stage, model geometry was created, numeric mesh generated and boundary conditions set. The numeric mesh consisted of about 3×10^5 tetrahedral cells. Mesh quality was examined by means of EquiAngle Skew and EquiSize Skew criterions [14]. Their values showed that the mesh had a good quality.

Numerical calculations and the analysis of results were carried out using the Ansys Fluent 14.0 solver and CFD Post post-processor, respectively. The base for calculations of discrete phase (particles) motion was the initial conditions, which determined the starting positions, velocity and other parameters for each stream of particles and physical effects affecting their stream. To simulate the motion of the discrete phase, the Euler–Lagrange (EL) [3] approach was used. In this approach, a motion of the continuous phase (gas) is modelled using the transport equations averaged over a computational cell and a discrete phase (particle) motion by solving the equations of motion for each particle separately.

Turbulent gas flow in the cyclone was described mathematically using the Navier–Stokes equations of mass and momentum transport, averaged further by the Reynolds method (RANS) [5]. As a closing method, the renormalization group (RNG) k - ε turbulence model was selected with an additional option of the swirl modification [15], taking into account the mean flow vorticity – vortex formation during polluted gas motion in our cyclone. The turbulence model complements with two basic equations such as equation of kinetic energy of turbulence k and that of the rate of energy dissipation ε . Detailed information on the method for gas flow modelling in the cyclone, the turbulence model and boundary conditions has been presented elsewhere [4].

4. RESULTS OF SIMULATION

Figure 3 presents visualizations of vortex formation for the selected gas flow velocity ($u = 15$ m/s). Visualizations were made on the basis of fixed values (iso-surfaces) of Q -criterion, defined as [16]:

$$Q = \frac{1}{2} (|\Omega|^2 - |S|^2) > 0 \quad (8)$$

where: S is the rate-of-strain tensor and Ω is the vorticity tensor.

The latter criterion was used to identify the cores of vortex structures, formed in the cyclone. On the basis of that it is possible to determine location and scale vortices generated in the dusty gas, involved in the dedusting process.

The images show two different structures of vortices, forming in the cyclone during gas flow: the main vortex (the outer spiral, where solid particles are separated) (Fig. 3a) with scale (diameter) comparable to the cylindrical part of the cyclone diameter, and a smaller-scale vortex (a stream of purified gas leaving the cyclone, the so-called inner spiral, Fig. 3b) with a diameter close to that of the vortex finder, forming in the cyclone center close to its vertical axis. Another interesting occurrence (Fig. 3a) was the formation of a chaotic gas flow in the dust chamber which can cause re-entrainment of the smallest particles that embedded earlier.

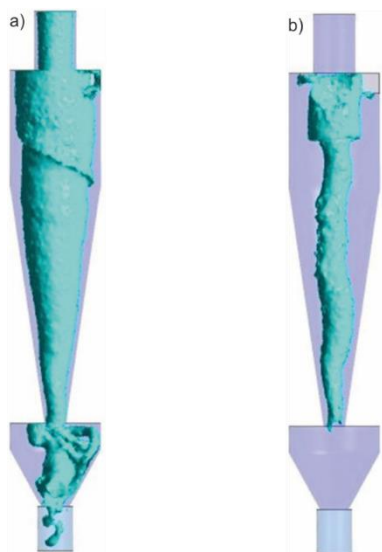


Fig. 3. Visualization of vortices in the cyclone using the Q -criterion:
a) the outer spiral ($Q = 0.45 \text{ s}^{-2}$), b) the inner spiral ($Q = 0.05 \text{ s}^{-2}$, $u = 15 \text{ m/s}$)

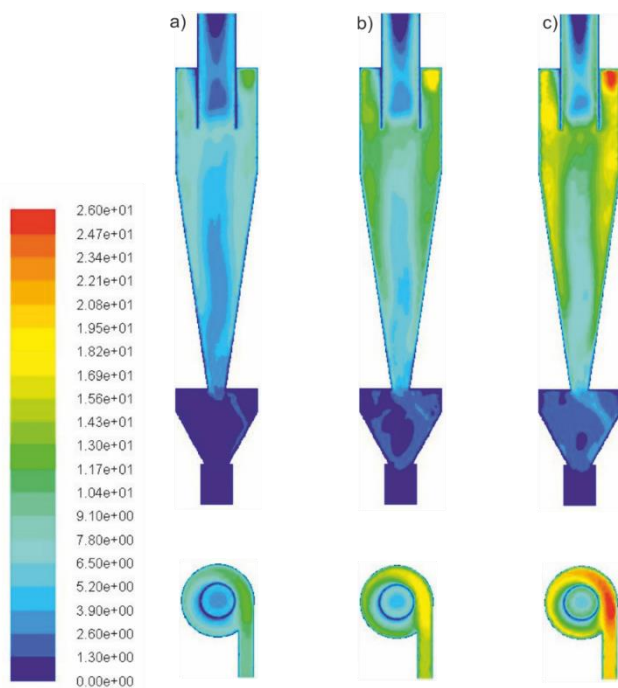


Fig. 4. Contour maps of gas velocities (m/s) in the cyclone for various inlet velocities:
a) $u = 10 \text{ m/s}$, b) $u = 15 \text{ m/s}$, c) $u = 20 \text{ m/s}$

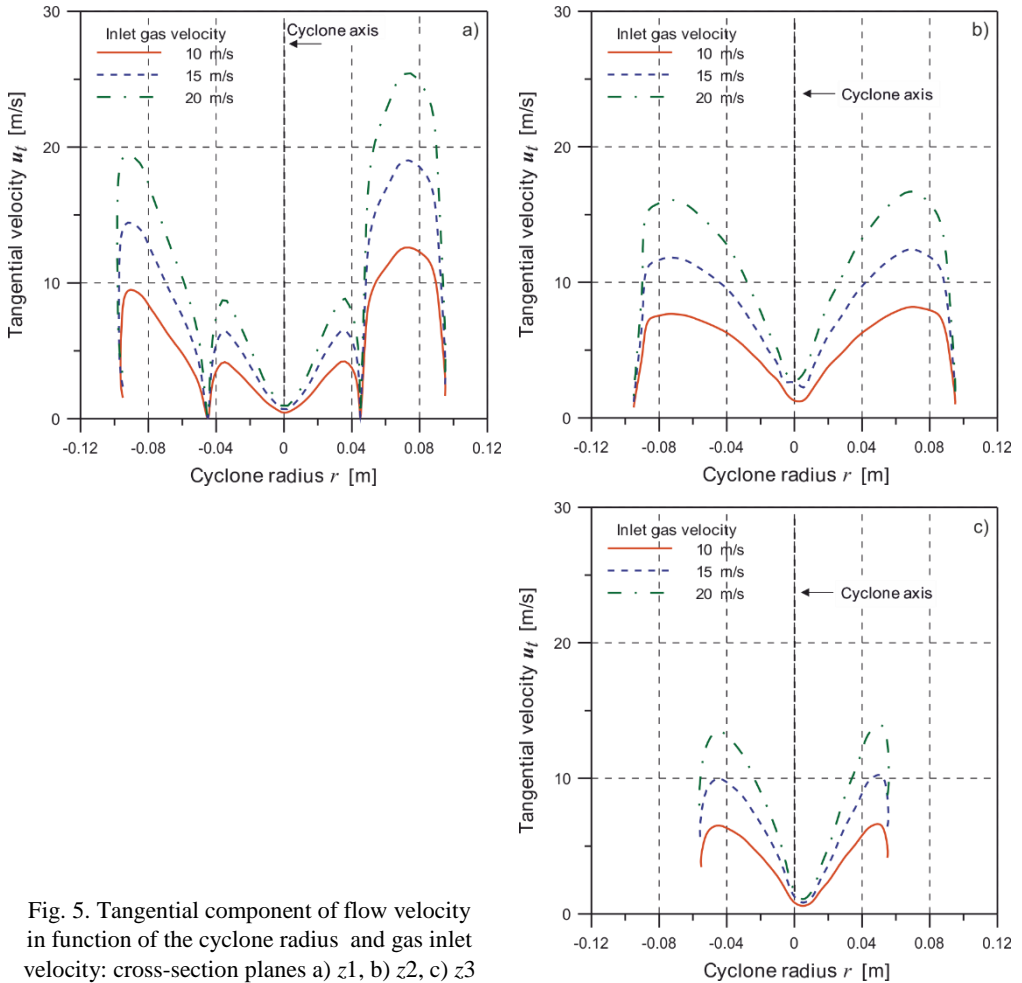


Fig. 5. Tangential component of flow velocity in function of the cyclone radius and gas inlet velocity: cross-section planes a) z_1 , b) z_2 , c) z_3

Another interesting phenomenon observed during simulations is high gas flow velocity at the connection of the inlet channel with the cylindrical part of the cyclone. Its qualitative analysis is presented in contour maps shown in Fig. 4 and a quantitative approach is illustrated in Fig. 5.

A detailed analysis shows that the reason for this may be a sudden narrowing of the gas stream at the start of its rotational motion and a high increase of the tangential component of velocity, crucial for a dedusting process. Its values can be higher than those of the gas inlet velocity even by 30% (Fig. 5a). This tendency was observed for all tested gas inlet velocities. It was reported and described elsewhere (cf. [4, 6]).

The analysis of curves illustrating changes of the tangential component velocity along cyclone radius for selected cutting cyclone planes (z_1 – inlet cross-section plane,

z_2 – cross-section plane in the zone of connection of a cylindrical part and conical ones, z_3 – cross-section plane in a half-height of conical part, Fig. 1) also showed that changes for z_1 plane are different from those, which are obtained for z_2 and z_3 . In this first case (Fig. 5a) we can see four maxima: two of them characterize the main flow in the cylindrical part of the cyclone, two characterize the flow in the vortex finder. The values of the gas velocity vary by 30–35% for the main flow, probably due to an increase of the flow velocity at the start of gas rotational motion. The values of the vortex finder maxima are comparable, pointing to a stable swirling flow in this zone.

For two other cross-section planes (Figs. 5b, c) profiles are very similar, differences are observed only in figures. A distinct maximum of velocity close to the cyclone wall is visible and its minimum in the vicinity of the cyclone vertical axis. This clearly indicates the existence of previously shown flow pattern that plays a decisive role in a de-dusting process and deposition of particles.

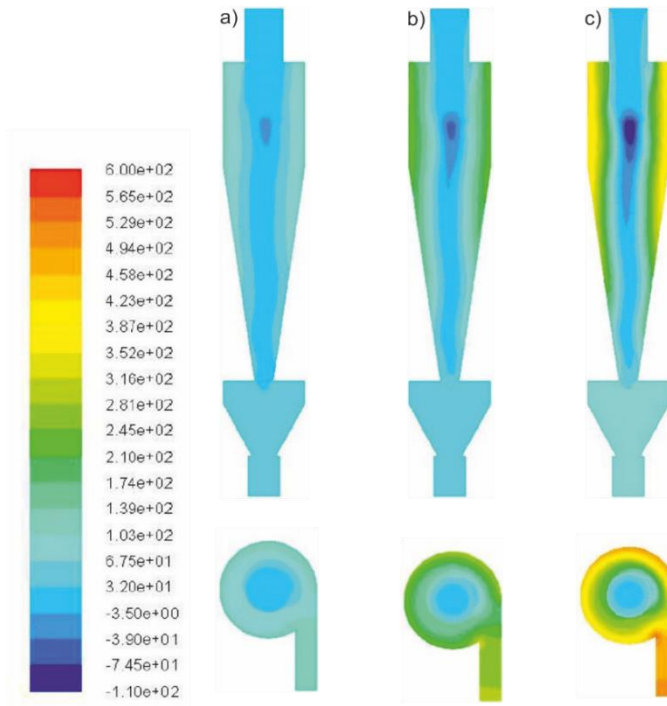


Fig. 6. Distribution of the static pressure (Pa) in the cyclone for various inlet velocities:
a) $u = 10$ m/s, b) $u = 15$ m/s, c) $u = 20$ m/s

Figure 6 shows a distribution of a static pressure in the cyclone for three gas inlet velocities $u = 10, 15, 20$ m/s. The values and distribution of the static pressure in the cyclone change substantially, depending on the gas velocity at the inlet. However, some trends are similar. The highest values of the static pressure are observed in the upper,

cylindrical part of the cyclone, particularly close to its wall. The smallest ones are in the cyclone interior, close to the axis. Narrow and relatively small zones of subatmospheric pressure are visible in the upper part of the cyclone at the beginning of the vortex finder.

Based on the simulated values of the static pressure, a pressure drop in the cyclone was calculated. It is one of the most important parameters characterizing cyclone performance and its operation costs. The pressure drop was calculated as the difference between the static pressures: at the inlet and in the vortex finder. Obtained results were compared with those measured in a real dedusting installation with a cyclone of similar geometry and dimensions (Fig. 1) [17]. A comparison of results is shown in Table 2.

Table 2

Pressure drop for the examined cyclone [Pa]

Inlet velocity [m/s]	Pressure drop according to Eqs.				CFD simulations		Measurements
	(1) $\alpha = \zeta = 6$	(1) and (2)	(1) and (3)	(1) and (4)	static pressure	total pressure	
10	367	203	213	216	134	169	190
15	826	459	480	284	313	366	340
20	1470	820	854	505	564	649	580

The differences between the values of pressure drops predicted by CFD simulations using static pressure values and those obtained from measurements were remarkably small. For gas inlet velocities $u = 15$ m/s and $u = 20$ m/s, they did not exceed 8.5% and 2.8%, respectively. Bigger difference (ca. 40%) was visible only for the lowest gas inlet velocity ($u = 10$ m/s) probably due to not sufficiently precise definition of the CFD model of cyclone operating parameters. Consequently, inaccuracies in the mathematical description of some geometrical quantities, e.g. sharp edges and surface roughness, might have had a more expressive effect at such low gas speeds.

The pressure drops determined with different models and correlations proposed in literature substantially differ. The highest values – significantly different from others – were determined from Eq. (1) using relatively low values of the coefficient $\alpha = \zeta = 6$, recommended for a cyclone of a similar geometry. The next two models (Eqs. (1) and (2), as well as Eqs. (1) and (3)) produced quite similar pressure drops, with slightly higher values than those of the approach described by Eq. (3). The lowest values of the pressure drop in the cyclone were obtained using Eqs. (1) and (4). Because these models consider the total (static and dynamic) pressure, for a better comparison, this quantity was predicted from simulations (Table 2). The smallest discrepancies between predicted and calculated values gives the Coker model (maximum differences do not exceed 28%) and this model seems to be the most useful to predict the pressure drop in the analyzed cyclone.

Figure 7 shows a visualization of a movement of hypothetical dust particles in the cyclone at the inlet gas velocity $u = 15$ m/s. Trajectories of particles were analyzed for three different particle diameters, 2, 20 and 100 μm . Particles were injected into the cyclone in the central point of the inlet channel (the intersection point of the diagonals of the square).

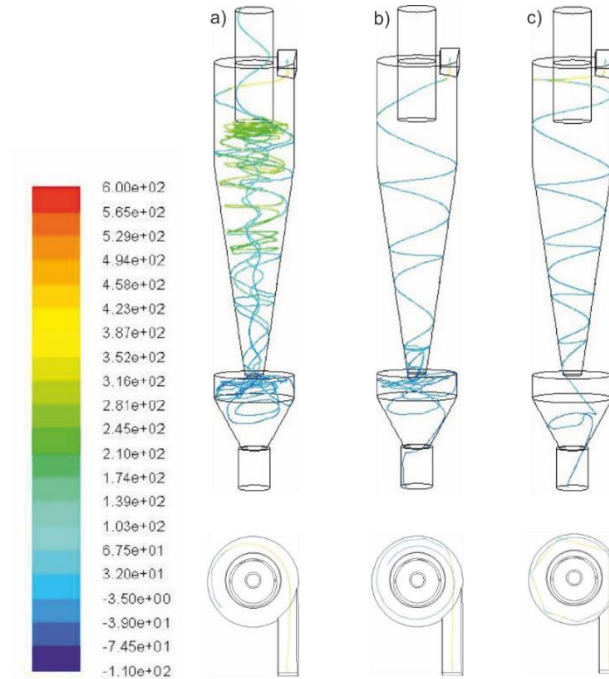


Fig. 7. Trajectories of particles of various diameters:
a) $d_p = 2 \mu\text{m}$, b) $d_p = 20 \mu\text{m}$, c) $d_p = 100 \mu\text{m}$ ($u = 15$ m/s)

The smallest particles (Fig. 7a) injected tangentially to the cyclone begin to move the swirl motion, creating an outer spiral with a large diameter. They lose their velocity as they come into contact with the wall in the cylindrical part of the apparatus. Next, with a slow velocity and swirling motion, they slide down to the dust chamber. The smallest particles are then re-entrained by the flow of the purified gas and with a swirling motion create an inner spiral, and eventually leave the cyclone along with the gas.

Larger particles, with a diameter d_p of approximately 20 μm (Fig. 7b) embed at the beginning of their movement and losing velocity with the spiral movement slide down to the dust chamber. Although at the top part of the chamber we can observe disturbances of their trajectories, they are separated from the polluted gas.

The largest particles ($d_p \approx 100 \mu\text{m}$) as a result of their inertia strike a wall of the cyclone already at the beginning of their movement (just after being inserted into the

cyclone), they can be reflected from the wall and next embed on the wall and slide down with a spiral movement into the dust chamber (Fig. 7c).

The above-described mechanism is directly related to the second parameter that influences the effectiveness of cyclone performance – dedusting efficiency. Software used in this study allows to monitor the number of particles: introduced, embedded and leaving the cyclone along with the purified gas, for a specified range of their diameters. Therefore, it is possible to calculate the mass of particles at the inlet and outlet of the cyclone, and also those that embed in the dust chamber. These data were used to calculate a dedusting efficiency of the cyclone, according to classic proportion (Eq. (5)). Results were compared to those calculated from a literature correlation (Eq. (6)) and those measured in a real installation (processed with Eq. (5)). A comparison is presented in Table 3.

Table 3

Calculated and simulated dedusting efficiencies of the cyclone [%]

Inlet velocity [m/s]	Efficiency of dedusting		
	According to Eq. (6)	CFD simulations	Measurements
10	80.3	80.8	83.3
15	84.3	86.3	87.8
20	86.9	87	91.2

Regardless of the gas inlet velocity, the obtained results are very similar, and in some cases almost identical. The maximum difference between simulated and calculated values does not exceed 2.3% and in the case of simulated and measured data is slightly higher, reaching 4.8%. This indicates the high quality of used the numerical model and its usefulness for determination of a dedusting efficiency of the cyclone.

5. CONCLUSION

The goal of the simulations was a numerical modeling of the two-phase (gas and solid) flow in the cyclone with a tangential inlet. During investigations the usefulness of the computer software to analyse cyclone performance was also examined. The results were compared with data calculated from empirical/literature correlations as well as the results of our own measurements.

Qualitative and quantitative analysis showed a relatively good consistence between data obtained from simulations, calculations and measurements. In the case of estimation of the pressure drop, the smallest differences were obtained during the comparison

of simulated and measured data with the Coker model. However, in the case of dedusting efficiency, simulated, calculated and measured data were almost identical, which confirms the selection of the applied numerical model.

The simulations showed also that computational packages based on CFD codes are a useful and effective tool which may be successfully used in the design and optimization of cyclones. They allow quick and easy analysis of polluted gas flow inside a cyclone without time-consuming experimental tests and building of prototypes. Moreover, with the use of CFD analysis we can also very quickly change and modify the geometry of the cyclone in a wide range variability of process parameters and – in consequence – improve the performance of apparatuses.

An inconvenience of the software used is its relatively poor database, including theoretical particle size distributions. This imposes some limitations in the use of CFD analysis for the description of diameters and particle size distributions of some dusts used in the industrial practice. Another disadvantage of used CFD software is its inability to simulate the interaction among solid particles which restricts the use of the model for a dusty gas with a low concentration of solid particles.

SYMBOLS

a, b	– inlet height and width of the cyclone, m
B	– diameter of the conical part, m
D	– diameter of the cyclone body, m
c	– length of the inlet channel, m
d_p	– particle diameter, μm
$d_{p\text{max}}$	– maximum particle diameter, μm
$d_{p\text{min}}$	– minimum particle diameter, μm
$d_{p\text{mn}}$	– mean particle diameter, μm
d_{32}	– Sauter mean particle diameter, μm
D_e	– vortex finder diameter, m
h	– height of the cylindrical part, m
H	– cyclone height, m
k	– turbulence kinetic energy, m^2/s^2
m_s	– mass of collected particles, kg
m_i	– mass of all particles introduced, kg
n	– total number of particles
n	– vortex exponent
r	– cyclone radius, m
R	– cyclone body radius, m
s	– vortex finder length (inside the cyclone), m
S	– rate-of-strain tensor, $1/\text{s}$
t	– time, s
T_p	– particle temperature, K
u	– gas inlet velocity, m/s
u_t	– gas tangential velocity, m/s
Q	– Q -criterion value, $1/\text{s}^2$

z_1, z_2, z_3	– cross-section planes
α	– cyclone dimensions coefficient
β	– spread parameter
Δp	– pressure drop, Pa
ε	– energy dissipation, m^2/s^3
η, η_i	– dedusting efficiency, %
μ_c	– continuous phase viscosity, $\text{Pa}\cdot\text{s}$
ξ	– local resistance coefficient
ρ_c	– continuous phase density, kg/m^3
ρ_s	– density of solid particle, kg/m^3
σ	– standard deviation, μm
τ	– response time, s
Ω	– vorticity tensor, $1/\text{s}$

REFERENCES

- [1] HOFFMANN A.C., STEIN L.E., *Gas cyclones and swirl tubes. Principles, design and operation*, Springer-Verlag, Berlin 2008.
- [2] WARYCH J., *Gas Cleaning*, WNT, Warsaw 1998 (in Polish).
- [3] ANDERSSON B., ANDERSSON R., HAKANSSON L., MORTENSEN M., SUDIYO R., VAN WACHEM B., *Computational Fluid Dynamics for Engineers*, Cambridge University Press, Cambridge 2012.
- [4] WÓJTOWICZ R., *Computer CFD simulations of gas flow in a radial cyclone*, *Czasop. Techn. – Techn. Trans.*, 2012, 2M, 485 (in Polish).
- [5] POPE S.B., *Turbulent Flows*, Cambridge University Press, Cambridge 2000.
- [6] ELSAYED K., LACOR C., *Optimization of the cyclone separator geometry for minimum pressure drop using mathematical models and CFD simulations*, *Chem. Eng. Sci.*, 2010, 65, 6048.
- [7] SAFIKANI H., AKHAVAN-BEHABADI M.A., SHAMS M., RAHIMYAN, *Numerical simulation of flow field in three types of standard cyclone separators*, *Adv. Powder Technol.*, 2010, 21, 435.
- [8] PAIVA J., SALCEDO R., ARAUJO P., *Impact of particle agglomeration in cyclones*, *Chem. Eng. J.*, 2010, 162.
- [9] SURMEN A., AVCI A., KARAMANGIL M.I., *Prediction of the maximum-efficiency cyclone length for a cyclone with a tangential entry*, *Powder Technol.*, 2011, 207, 1.
- [10] CASAL J., MARTINEZ J.M., *A better way to calculate cyclone pressure drop*, *Chem. Eng.*, 1983, 90, 99.
- [11] SHEPHERD C.B., LAPPLE C.E., *Air pollution control: a design approach*, [in:] C.D. Cooper, F.C. Alley (Eds.), *Cyclones*, Woveland Press, Inc., Illinois 1939.
- [12] COKER A.K., *Understand cyclone design*, *Chem. Eng. Progr.*, 1993, 28, 51.
- [13] LICHT W., *Air Pollution Control Engineering*, Marcel Dekker, New York 1992.
- [14] *Gambit 2.4 User's Guide*, Ansys., Inc., Lebanon, 2009.
- [15] *Ansys Fluent 14.0 Theory Guide*, Ansys Inc., Lebanon, 2011.
- [16] HUNT J.C.R., WRAY A.A., MOIN P., *Eddies, streams and convergence zones in turbulent flow*, *CTR-S88*, 1988, 193.
- [17] Unpublished data, Division of Industrial Equipment, Cracow University of Technology, Cracow 2014.